

14.1 NUMERICAL SIMULATION OF A CYCLIC TORNADIC THUNDERSTORM AUGMENTED BY EnKF ASSIMILATION OF MOBILE DOPPLER RADAR DATA

Robin L. Tanamachi*
*School of Meteorology, University of
Oklahoma (OU), Norman, Oklahoma*

David C. Dowell
*National Center for Atmospheric Research
(NCAR), Boulder, Colorado*

Louis J. Wicker
*National Severe Storms Laboratory, Norman,
Oklahoma*

Howard B. Bluestein
*School of Meteorology, University of
Oklahoma (OU), Norman, Oklahoma*

Stephen J. Frasier
*Microwave Remote Sensing Laboratory
(MIRSL), University of Massachusetts –
Amherst, Amherst, Massachusetts*

Kery Hardwick
Northampton, Massachusetts

1. INTRODUCTION

Radar is one of few atmospheric measurement tools capable of collecting volumetric data at temporal and spatial scales at which sub-storm scale features can be discerned and tracked. As such, assimilation of radar data into numerical weather prediction (NWP) models with the goal of improved understanding of storm dynamics is now a fairly routine exercise, and prediction of high-impact, sub-storm scale features such as tornadoes is a natural objective (Dawson and Xue 2006; Hu and Xue 2007; Dawson *et al.* 2008; Aksoy *et al.* 2009; Dowell and Wicker 2009).

Two measured radar variables are most often assimilated into NWP models: Doppler velocity and reflectivity. NWP models require and calculate additional variables, such as temperature and pressure, that radar observations alone do not furnish. As a potential pathway toward alleviating this underdetermined problem, the ensemble Kalman filter (EnKF) (Evensen 1994; Houtekamer and Mitchell 1998) has been used in previous studies to infer the temperature and pressure fields based, at least in part, on Doppler radar measurements (Snyder and Zhang 2003; Dowell *et al.* 2004a; Dowell *et al.* 2004b; French *et al.* 2006; Aksoy *et al.* 2009; Dowell and Wicker 2009).

The objective of the following study is to assess the added impact (relative to assimilation of WSR-88D observations only) of assimilation of mobile Doppler radar observations collected in the 4 May 2007

Greensburg, Kansas tornadic thunderstorm (hereafter “the Greensburg storm”) into the Weather Research and Forecasting (WRF) NWP model via the EnKF technique. In particular, it is expected that the additional assimilation of relatively high-resolution mobile Doppler radar data will result in a more accurate reproduction of the mesocyclone and tornado tracks in the storm, which are highly dependent upon the air flow fields at low levels. Ultimately, it is hoped that higher-resolution versions of this experiment will illuminate the internal dynamics of the Greensburg storm, particularly its transition from a cyclic tornadic phase to a relatively long-track tornadic phase.

2. THE GREENSBURG TORNADIC STORM

On 5 May 2007 (UTC time, 4 May 2007 local time), a cyclic tornadic supercell produced an EF-5 tornado (hereafter “the Greensburg tornado”) at 0200 UTC and severely damaged the town of Greensburg, Kansas around 0245 UTC. The tornado damage path was 53 km in length and 3.1 km wide at its widest point (Lemon and Umscheid 2008). The Greensburg tornado was preceded by four smaller (EF-0 and EF-1) tornadoes, and the Greensburg storm continued producing significant tornadoes for over an hour after the Greensburg tornado dissipated at 0300 UTC. Lemon and Umscheid (2008) and Bluestein (2009) have extensively documented the meteorological aspects of the Greensburg storm and its environment.

3. RADAR DATA

Radar reflectivity and Doppler velocity data were collected in the Greensburg storm by both the Dodge City, Kansas WSR-88D (KDDC) (Lemon and Umscheid 2008;

* Corresponding author: Robin L. Tanamachi; Univ. of Oklahoma; School of Meteorology; 120 David L. Boren Blvd., Suite 5900; Norman, OK 73072-7307; e-mail: rtanamachi@ou.edu

Bluestein 2009) and the University of Massachusetts mobile, X-band, dual-polarization Doppler radar (UMass X-Pol) (Bluestein *et al.* 2007).

KDDC collected volumetric radar data in “precipitation mode” (Volume Coverage Pattern 12) every 4.1 min throughout the duration of the Greensburg storm (Fig. 1). It can be seen in the KDDC data that the Greensburg storm had a classic supercell structure with a precipitation-filled hook region on its southwest flank.

As part of a severe thunderstorm research project (Bluestein *et al.* 2007), UMass X-Pol was deployed 4 km east of the town of Protection, KS, about 48 km south-southwest of Greensburg. One hundred and six single-elevation sector scans were collected at low elevation angles (3 – 5 deg) from 0115 to 0126 UTC, focusing primarily on the hook region of the Greensburg storm. A total of 81 volume scans, with elevation angles ranging from 3.0° to 10°, 15°, or 20°, were collected with a frequency ~ 1 min from 0126 to 0236 UTC (except for a six-minute gap when the truck was moved a short distance in order to minimize beam blockage). UMass X-Pol had to be shut down at 0236 UTC owing to low onboard battery power; recall that Greensburg was initially struck by the EF-5 tornado at around 0245 UTC. Fig. 2 summarizes the timeline of the Greensburg radar data collection.

The supercell structure and tornadic region of the Greensburg storm are evident in UMass X-Pol data from 0231 UTC (Fig. 3). Measured velocities at 1.0 km AGL in the Greensburg tornado exceeded 60 m s⁻¹. Dual-polarization measurements (not shown) were used to infer the location of the Greensburg tornado debris column (Bluestein *et al.* 2008), but these data were not used in the following assimilation study.

4. METHODOLOGY

The complementary spatial and temporal coverage of the same tornadic storm by two sets of independently-gathered radar data make these data an attractive candidate for a data assimilation study. The following experiments follow a methodology similar to those of Dowell and Wicker (2009) and Aksoy *et al.* (2009).

Prior to objective analysis, the Doppler velocity data from both the KDDC and UMass X-Pol radars were manually dealiased. In

addition, a reflectivity threshold of 0 dBZ was applied to the UMass X-Pol Doppler velocity data, and regions of second-trip echo and ground clutter were manually removed from both the reflectivity and Doppler velocity data. (See Fig. 3[c] for an example.)

In the objective analysis, each radar data range gate was treated as a point observation, and the points remained on their original sweep surfaces while being interpolated horizontally to a 2 km Cartesian grid using a single-pass Barnes scheme (Trapp and Doswell 2000). This procedure preserved the relative density of observations in the vertical near each radar. An example objective analysis is shown in Fig. 4.

We simulated the Greensburg storm using the Weather Research and Forecasting (WRF, <http://www.wrf-model.org>) NWP model version 3.0.1.1 (Skamarock *et al.* 2008). We used the EnKF radar data assimilation module of the Data Assimilation Research Testbed (DART, <http://www.image.ucar.edu/DAReS/DART>) package (Anderson and Collins 2007), to assimilate radar data into the WRF model.

We employed a 124 km × 124 km × 20 km simulation domain centered roughly on Greensburg, Kansas (37.602 °N, 99.292 °W). The grid had 2 km horizontal grid spacing and slightly non-uniform vertical grid spacing (~400 m over 51 vertical levels) from 650 m (the model bottom boundary) to 20 km ASL.

For cloud and precipitation microphysics, the single-moment Purdue Lin (1983) microphysical scheme in WRFV3 (Skamarock *et al.* 2008) was used. This scheme uses six hydrometeor classes, including three ice classes (cloud ice, snow, and hail/graupel). Hail was documented in the Greensburg storm (Lemon and Umscheid 2008), so a relatively high graupel density ($\rho_h = 917 \text{ kg m}^{-3}$) and slope intercept parameter ($N_{0h} = 40000 \text{ m}^{-4}$) were prescribed (Lin *et al.* 1983). No surface fluxes, turbulence parameterizations, or radiation physics were used.

The initial model state was derived from a modified version of the 0000 UTC rawinsonde from Lamont, Oklahoma (LMN; Fig. 5). The LMN sounding was selected because it was felt to be representative of the inflow environment of the Greensburg storm. (The nearer 0000 UTC Dodge City, Kansas [DDC] sounding was taken behind an advancing dryline.) The following modifications were made to the LMN sounding: (1) the sounding was truncated at the model bottom boundary

(650 m ASL); (2) the surface temperature, dewpoint, and wind observations from Pratt, Kansas (KPTT, 50 km east of Greensburg) were inserted at the level of the model bottom boundary; (3) a well-mixed (constant- θ , constant- q_v) layer, with values equal to the KPPT observation ($\theta = 306.7$ K, $q_v = 15.0$ g kg⁻¹), was substituted in the lowest 1500 m; and (4) within this well-mixed layer, the wind directions (but not speeds) were adjusted so that the 0 - 1 km wind shear in the Greensburg storm inflow environment would be realized on the lowest two model levels. This modified Lamont sounding exhibited CAPE ~4800 J kg and 22 m s⁻¹ 0-6 km vertical shear (Fig. 6), which are both consistent with an environment supportive of supercell thunderstorms.

An ensemble of 48 model initial states was populated by adding random perturbations $\sim N(0 \text{ m s}^{-1}, [2.0 \text{ m s}^{-1}]^2)$ to both the u and v wind components in the modified LMN sounding. The temperature profile was *not* perturbed so as to avoid the inadvertent generation of superadiabatic layers. These 48 perturbed soundings were then interpolated to the model vertical levels in order to generate the horizontally homogeneous initial model states.

Radar data were assimilated every 2 min over the time period 0030 to 0300 UTC on 5 May 2007, encompassing the interval when data from both radars were available. (Recall Fig. 2.) In contrast to previous data assimilation studies of the Greensburg case, e.g., (Gao *et al.* 2008), no observations other than those from the two radars were assimilated. An additive noise scheme (Caya *et al.* 2005; Dowell and Wicker 2009), in which random noise was added to the model temperature, moisture, and horizontal velocity fields in areas where KDDC reflectivity was > 25 dBZ, was applied at each analysis time, and the model advanced, using a time step of 5 s, to the next analysis time. Unlike previous radar data assimilation studies, e.g., Dowell *et al.* (2004a), no thermal bubbles were used to initiate the storm updrafts.

Within the above framework, we performed the following two experiments:

- **KDDC_only:** Low reflectivity and Doppler velocity data from KDDC were assimilated.
- **KDDC_UMass:** Same as KDDC_only, but Doppler velocity data from UMass X-Pol were also assimilated.

The KDDC low reflectivity data were assimilated in order to suppress spurious

convection in the model. In this instance, “low reflectivity” refers to reflectivity values ≤ 0 dBZ. KDDC high reflectivity (> 0 dBZ) data were not assimilated in these experiments (although they were used to calculate the additive noise fields). UMass X-Pol reflectivity data were withheld from assimilation because of significant attenuation of the X-band signal by hail in the core of the Greensburg storm (Fig. 3), and because the reflectivity forward operator in DART was formulated for S-band reflectivity, not X-band.

5. RESULTS

Examples of the prior ensemble mean analysis fields at 0230 UTC (when the Greensburg tornado was mature) for the KDDC_only and KDDC_UMass experiments are shown in Fig. 7. It can be seen that, in both experiments, the model produces a storm with a rotating updraft that follows the same track as the Greensburg storm. However, the KDDC_only storm appears to possess a double-updraft structure at 4 km AGL, whereas the KDDC_UMass storm possesses a single, larger updraft. The reflectivity core, mid-level updraft, and (particularly) low-level vorticity maximum associated with the Greensburg storm in the KDDC_UMass experiment are stronger than those in the KDDC_only experiment. We infer that the additional information imparted to the model via assimilation of the more frequently-collected, higher-resolution UMass X-Pol velocity data increased the intensity of these analyzed features in the Greensburg storm, as one might expect.

We note, however, that the ensemble mean analysis increments (posterior – prior; not shown) for vertical velocity sometimes exceed +10 m s⁻¹ in both experiments, particularly between 0200 and 0230 UTC. From examination of vertical velocity fields from individual ensemble members (not shown), we infer that the EnKF effects a significant adjustment to the 2-min model forecasts, and that the presence of the updraft within the analysis results mainly from the assimilation of the Doppler velocity observations and not from persistence of the updraft within the model. The maximum theoretical updraft strength (not accounting for the effects of vertical perturbation pressure gradient force, entrainment, or precipitation loading) supported by the modified LMN

sounding ($w_{\max} = \sqrt{2 * CAPE}$) is 97 m s^{-1} .

The updraft strength in the model never exceeds 55 m s^{-1} , possibly owing to the relatively coarse horizontal (2 km) and vertical resolution (~400 m) of the model grid at low levels.

In both experiments, extensive cold pools (not shown) are produced by the simulated Greensburg storm. However, the coverage and coldness of the cold pool is more limited in the KDDC_UMass experiment than in the KDDC_only experiment. Again, we infer that the added low-level velocity information from the UMass X-Pol radar serves to constrain the coverage and depth of the cold pool of the simulated Greensburg storm. However, we again caution that the coarse model resolution at low levels may limit the applicability of this result.

Some observation-space diagnostics (Dowell and Wicker 2009) from these experiments are shown in Fig. 8. It can be seen that, in the KDDC_UMass experiment, the layer-averaged innovation (model minus observation) decreases relative to the KDDC_only experiment over the 0 – 1000 m ASL layer during 0115 – 0126 UTC, when only single-elevation scans were being collected at low elevation angles (~ 3 - 4°; recall Fig. 2). During this period, ~ 20 single-elevation scans are assimilated over each 2 min cycle, so the observations are given much greater weight in the assimilation than the model velocity fields and the near-surface velocity fields more constrained in the model from cycle to cycle. Similar improvement to the innovation can be seen over the 3000 – 4000 m layer, particularly after UMass X-Pol volume scans begin at 0127 UTC (Fig. 2). The innovation in this layer decreases to near zero when the maximum elevation angle in the volume scans increased to 20° from 0225 – 0236 UTC. Strangely, in the 0 – 1000 m layer, the innovation increases after volume scans begin at 0127 UTC. The reason for this reversal in the sign of the effect is unclear, but we speculate that the addition of UMass X-Pol data at higher elevations may alter the model air flow at these levels sufficiently enough to, in turn, modify the near-surface velocities such that they are inconsistent with the near-surface UMass observations.

The consistency ratio (CR), which is a measure of similarity between the ensemble statistics and the observation errors and

should nominally be close to 1.0, for these experiments was close to 1.0 over the 0 – 1000 m model level at almost all times during the experiment. However, CR was less than 1.0 at almost all model heights above 1000 m and all times, indicating too little model spread for most of the experiment. Methods of increasing the model spread at these levels (such as increasing the magnitude of the additive noise) are currently being explored.

6. DISCUSSION AND FUTURE WORK

Doppler velocity data from a WSR-88D and an X-band, mobile Doppler radar, along with low-reflectivity data from the WSR-88D, were assimilated into the WRF NWP model in an effort to simulate a cyclic tornadic supercell. The analyses appear to accurately place the supercell updraft, and the additional assimilation of UMass X-Pol data adds useful information about low-level wind fields. However, aspects of the experimental configuration may limit the usefulness of these results. First, the horizontal resolution of the model (2 km) is too coarse to resolve individual tornadoes, although the mesocyclone that produced the Greensburg tornado was itself of tornadic strength (Lemon and Umscheid 2008). Second, the vertical resolution of the model (~400 m) is far too coarse at low levels to resolve aspects of the environment such as the low-level vertical wind shear, that have been identified as critical to tornadogenesis.

Third, the experimental setup does not allow for a time-varying storm inflow environment (except for those variations produced by the model itself). It is believed that the initial model state, which was constructed to be representative of the storm inflow environment at 0000 UTC, became less representative of the inflow environment at later analysis times. In particular, the intensification of the nocturnal 850 mb southerly jet may have had a significant effect on the evolution of the Greensburg storm (Bluestein 2009). The intensification of the 850 mb jet can be clearly seen in the KDDC velocity data in Fig. 1. Efforts to reconstruct the storm inflow environment at times between 0100 and 0300 UTC are underway.

The higher spatial (150 m range gate spacing) and temporal (~ 1 min volume scans) resolution of the UMass X-Pol radar data (relative to those from KDDC) could be more fully exploited by higher-resolution versions of

the experiments described herein. Experiments in which the model has smaller horizontal and vertical grid spacing are planned; more frequent data assimilation cycles will be necessary as the horizontal grid resolution increases. It is hoped that higher-resolution versions of these experiments will illuminate the cyclic-to-long track tornadic phase of the Greensburg storm.

7. ACKNOWLEDGMENTS

The National Science Foundation (NSF) supported this study under NSF grant ATM-0637148. Donald J. Giuliano (Center for Analysis and Prediction of Storms) furnished archived NAM forecasts. Ted Mansell (NSSL) provided computing support. Mike Umscheid (NWS – Dodge City, Kansas) and Les Lemon (NWS – Warning Decision Training Branch) provided damage survey information, and much helpful discussion about the meteorological background of this case. Conversations with Glen Romine (NCAR) about the DART system and interpretation of the results were invaluable.

8. REFERENCES

- Aksoy, A., D. C. Dowell, and C. Snyder, 2009: A Multicase Comparative Assessment of the Ensemble Kalman Filter for Assimilation of Radar Observations. Part I: Storm-Scale Analyses. *Mon. Weather Rev.*, **137**, 1805-1824.
- Anderson, J. L., and N. Collins, 2007: Scalable Implementations of Ensemble Filter Algorithms for Data Assimilation. *Journal of Atmospheric and Oceanic Technology*, **24**, 1452-1463.
- Bluestein, H. B., 2009: The Formation and Early Evolution of the Greensburg, Kansas, Tornadic Supercell on 4 May 2007. *Weather and Forecasting*, **24**, 899-920.
- Bluestein, H. B., K. Hardwick, M. Umscheid, R. L. Tanamachi, J. B. Houser, and S. Frasier, 2008: Polarimetric-radar signatures associated with the Greensburg, Kansas tornado. *24th Conference on Severe Local Storms*, Savannah, Georgia, American Meteorological Society, 2.5. [Recorded presentation].
- Bluestein, H. B., and Coauthors, 2007: Preliminary results from the fielding of a disparate triad of mobile Doppler radars to study severe convective storms. *33rd International Conference on Radar Meteorology*, American Meteorological Society, 13A.12.
- Caya, A., J. Sun, and C. Snyder, 2005: A Comparison between the 4DVAR and the Ensemble Kalman Filter Techniques for Radar Data Assimilation. *Mon. Weather Rev.*, **133**, 3081-3094.
- Dawson, D. T., and M. Xue, 2006: Numerical Forecasts of the 15-16 June 2002 Southern Plains Mesoscale Convective System: Impact of Mesoscale Data and Cloud Analysis. *Mon. Weather Rev.*, **134**, 1607-1629.
- Dawson, D. T., M. Xue, and J. A. Milbrandt, 2008: Improvements in the treatment of evaporation and melting in multi-moment versus single-moment bulk microphysics: results from numerical simulations of the 3 May 1999 Oklahoma tornadic storms. *24th Conference on Severe Local Storms*, American Meteorological Society, 17B.14.
- Dowell, D. C., and L. J. Wicker, 2009: Additive Noise for Storm-Scale Ensemble Data Assimilation. *Journal of Atmospheric and Oceanic Technology*, **26**, 911-927.
- Dowell, D. C., L. J. Wicker, and D. J. Stensrud, 2004a: High resolution analyses of the 8 May 2003 Oklahoma City storm. Part II: EnKF data assimilation and forecast experiments. *22nd Conference on Severe Local Storms*, American Meteorological Society, 12.15.
- Dowell, D. C., F. Zhang, L. J. Wicker, C. Snyder, and N. A. Crook, 2004b: Wind and Temperature Retrievals in the 17 May 1981 Arcadia, Oklahoma, Supercell: Ensemble Kalman Filter Experiments. *Mon. Weather Rev.*, **132**, 1982-2005.
- Evensen, G., 1994: Sequential data assimilation with a nonlinear quasi-geostrophic model using Monte Carlo methods to forecast error statistics. *Journal of Geophysical Research*, **99**, 10143-10162.
- French, M. M., H. B. Bluestein, D. C. Dowell, L. J. Wicker, M. R. Kramar, and A. L. Pazmany, 2006: The 15 May 2003 Shamrock, Texas, supercell: A dual-Doppler analysis and EnKF data-assimilation experiment. *23rd Conference on Severe Local Storms*, American Meteorological Society, 14.16A.
- Gao, J., D. J. Stensrud, and M. Xue, 2008: Importance of Environmental Variability to

- Storm-scale Radar Data Assimilation. *24th Conference on Severe Local Storms*, American Meteorological Society, 9B.2.
- Houtekamer, P. L., and H. L. Mitchell, 1998: Data Assimilation Using an Ensemble Kalman Filter Technique. *Mon. Weather Rev.*, **126**, 796-811.
- Hu, M., and M. Xue, 2007: Impact of Configurations of Rapid Intermittent Assimilation of WSR-88D Radar Data for the 8 May 2003 Oklahoma City Tornadoic Thunderstorm Case. *Mon. Weather Rev.*, **135**, 507-525.
- Lemon, L. R., and M. Umscheid, 2008: The Greensburg, KS tornadoic storm: a storm of extremes. *24th Conference on Severe Local Storms*, American Meteorological Society, 2.4.
- Lin, Y.-L., R. D. Farley, and H. D. Orville, 1983: Bulk Parameterization of the Snow Field in a Cloud Model. *Journal of Applied Meteorology*, **22**, 1065-1092.
- Skamarock, W. C., and Coauthors, 2008: A description of the Advanced Research WRF Version 3, 113 pp.
- Snyder, C., and F. Zhang, 2003: Assimilation of Simulated Doppler Radar Observations with an Ensemble Kalman Filter. *Mon. Weather Rev.*, **131**, 1663-1677.
- Trapp, R. J., and C. A. Doswell, 2000: Radar Data Objective Analysis. *Journal of Atmospheric and Oceanic Technology*, **17**, 105-120.

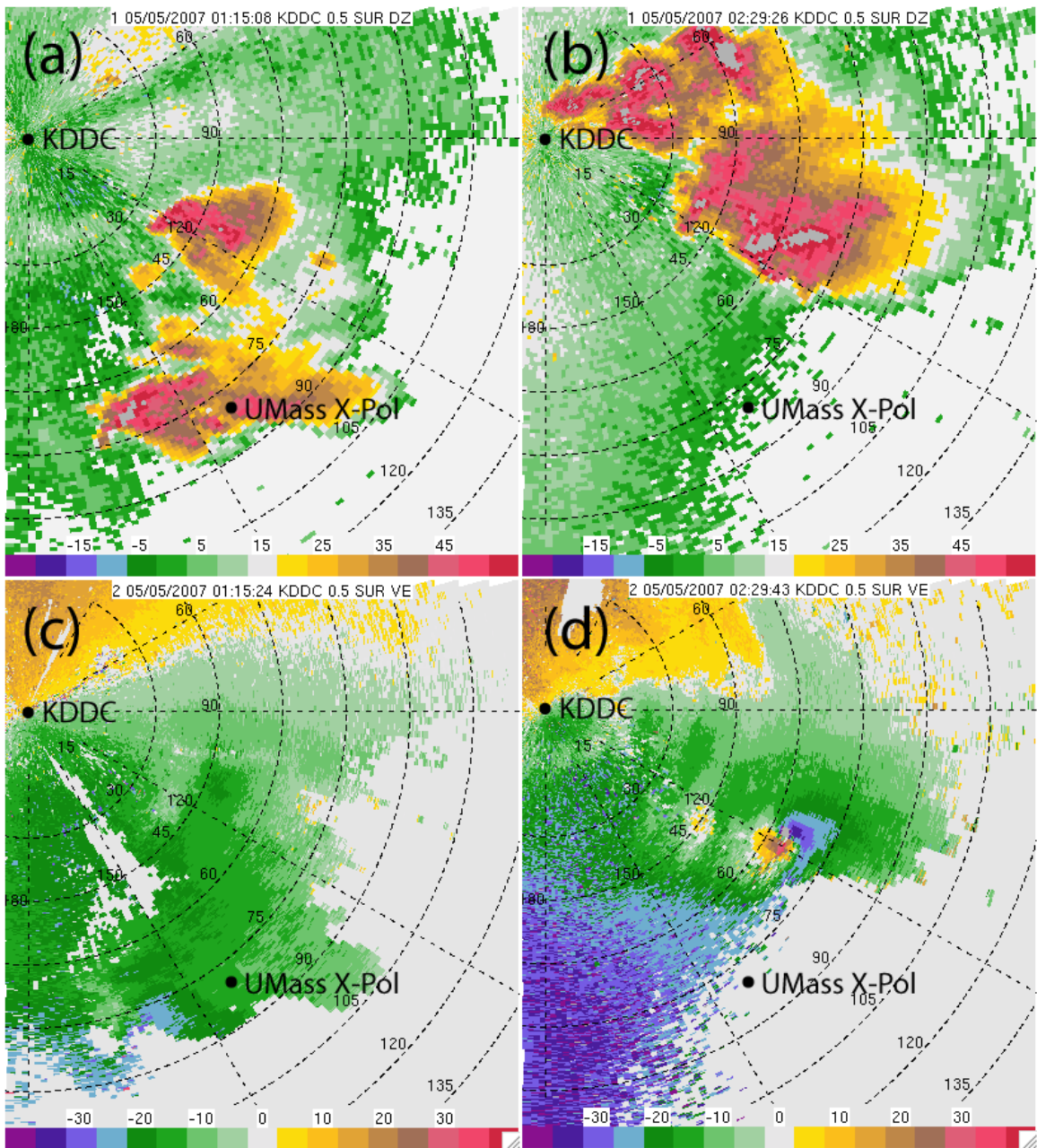


Fig. 1. (a,b) Reflectivity (in dBZ) and (c,d) manually dealiased Doppler velocity (in m s^{-1}), at an elevation angle of 0.5° , from the Dodge City, Kansas WSR-88D radar (located at the origin). Panels (a) and (c) are from 0115 UTC on 5 May 2007, and (b) and (d) are from 0229 UTC. At both times, the Greensburg storm is the southernmost storm. Range rings are 15 km apart, spokes are every 30 degrees. Black dots denote the locations of the KDDC and UMass X-Pol radars.

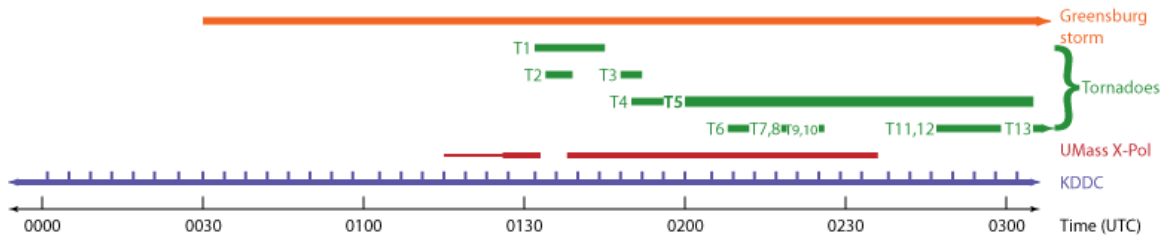


Fig. 2. Timeline of the Greensburg case on 5 May 2007, showing the life span of the Greensburg storm (orange line), life spans of tornadoes produced by the Greensburg storm (green lines; numbering convention is that of Lemon and Umscheid [2008] and T5 corresponds to the Greensburg tornado), UMass X-Pol data coverage (thin red line - single-elevation scans; thick red line - volume scans), and KDDC data coverage (purple line; tick marks indicate the start times of radar volumes).

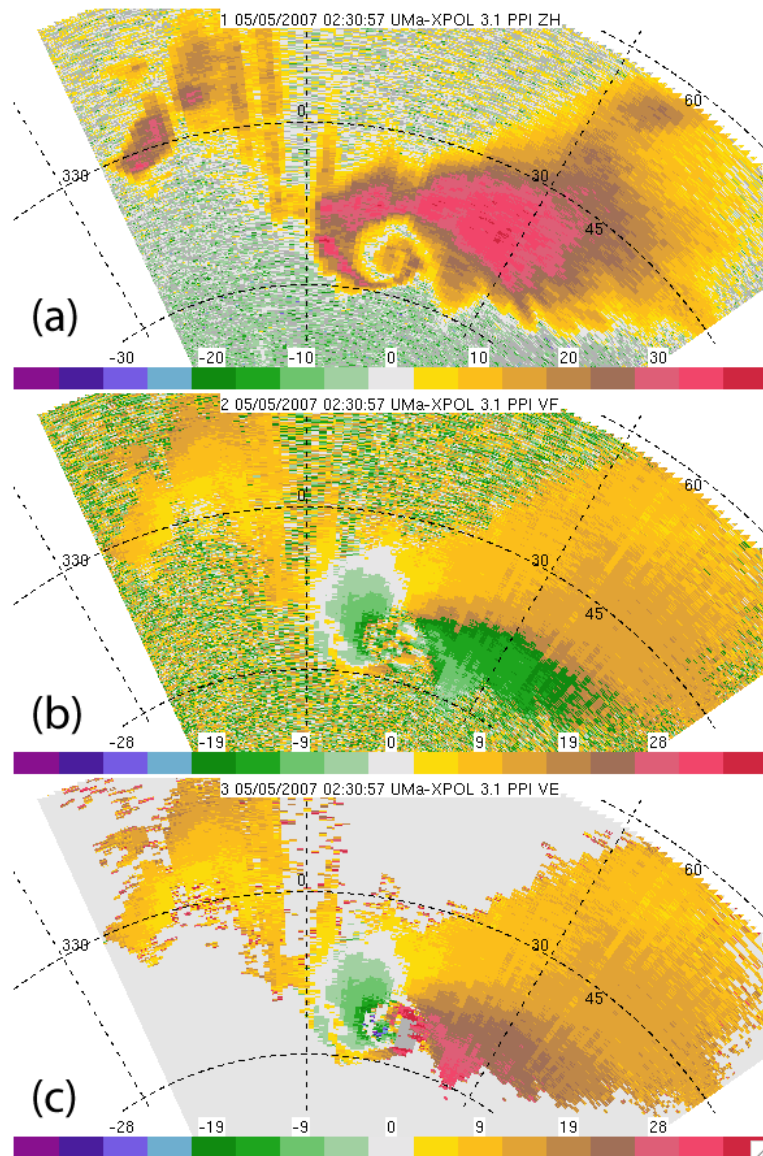


Fig. 3. (a) UMass X-Pol reflectivity (in dBZ) and (b) Doppler velocity (in m s⁻¹) at 0231 UTC, when the Greensburg tornado was mature. Range rings are 15 km apart; spokes are every 30 degrees. Manually dealiased and edited Doppler velocities appear in panel (c); the editing procedure is described in section 4.

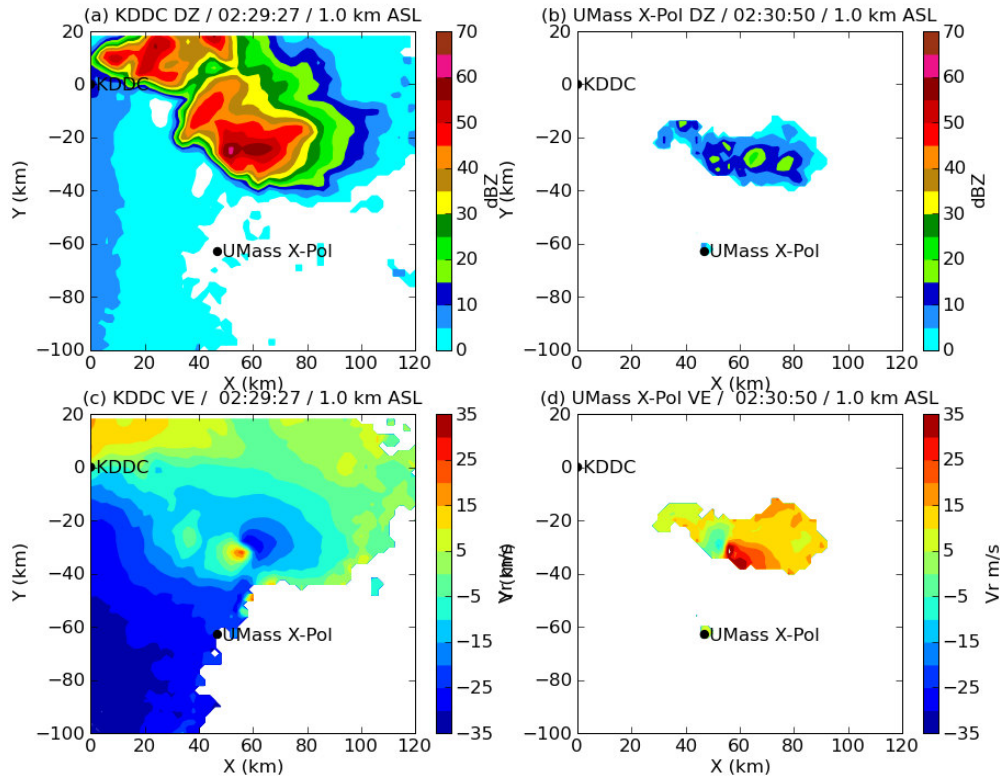


Fig. 4. Cartesian objective analyses of reflectivity (top row) and Doppler velocity (bottom row) from (a, c) KDDC and (b, d) UMass X-Pol at 1.0 km ASL from 0230 UTC on 5 May 2007. The grid origin is located at KDDC. The differences in reflectivity likely from the different calibration methods used for the two radars.

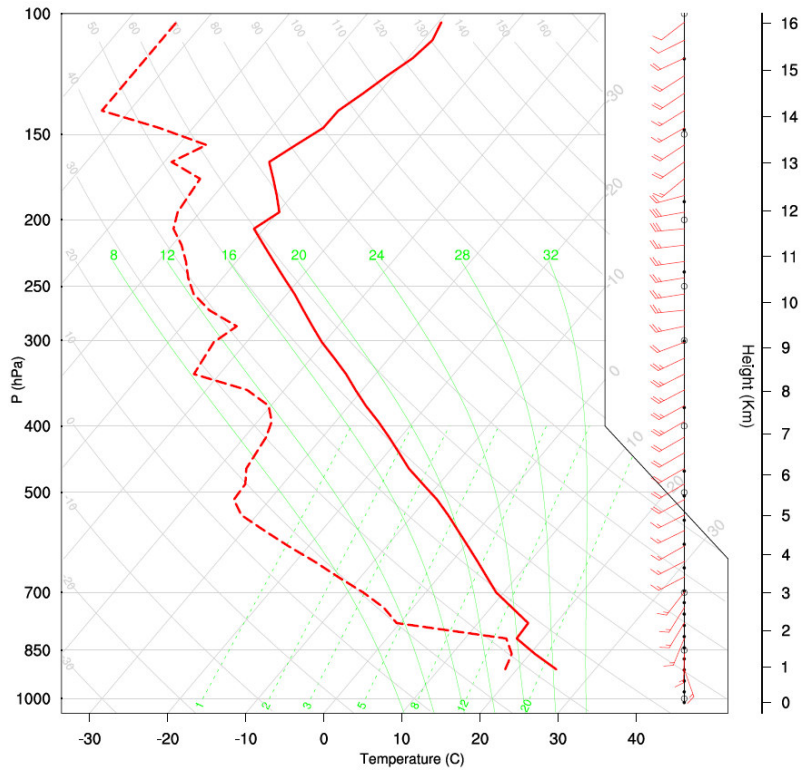


Fig. 5. Modified Lamont, Oklahoma sounding used to initialize the data-assimilation experiments. Wind barbs are in m s^{-1} .

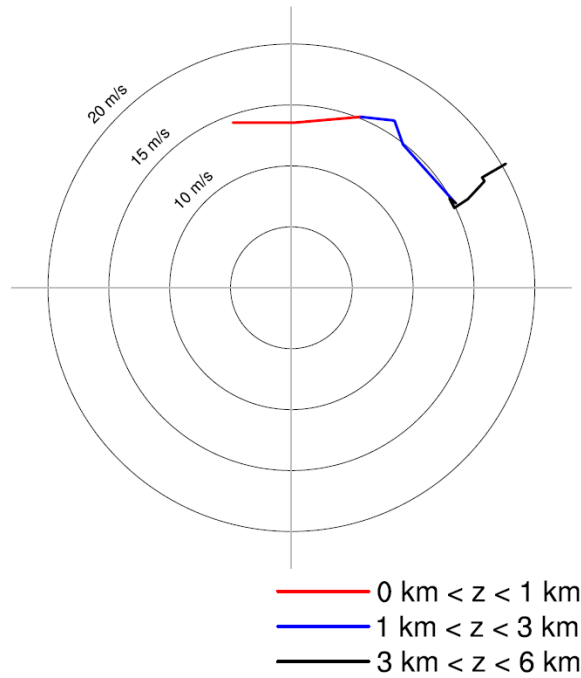


Fig. 6. Hodograph corresponding to Fig. 5. The lowest level plotted is 878 m ASL, the lowest scalar level of the model.

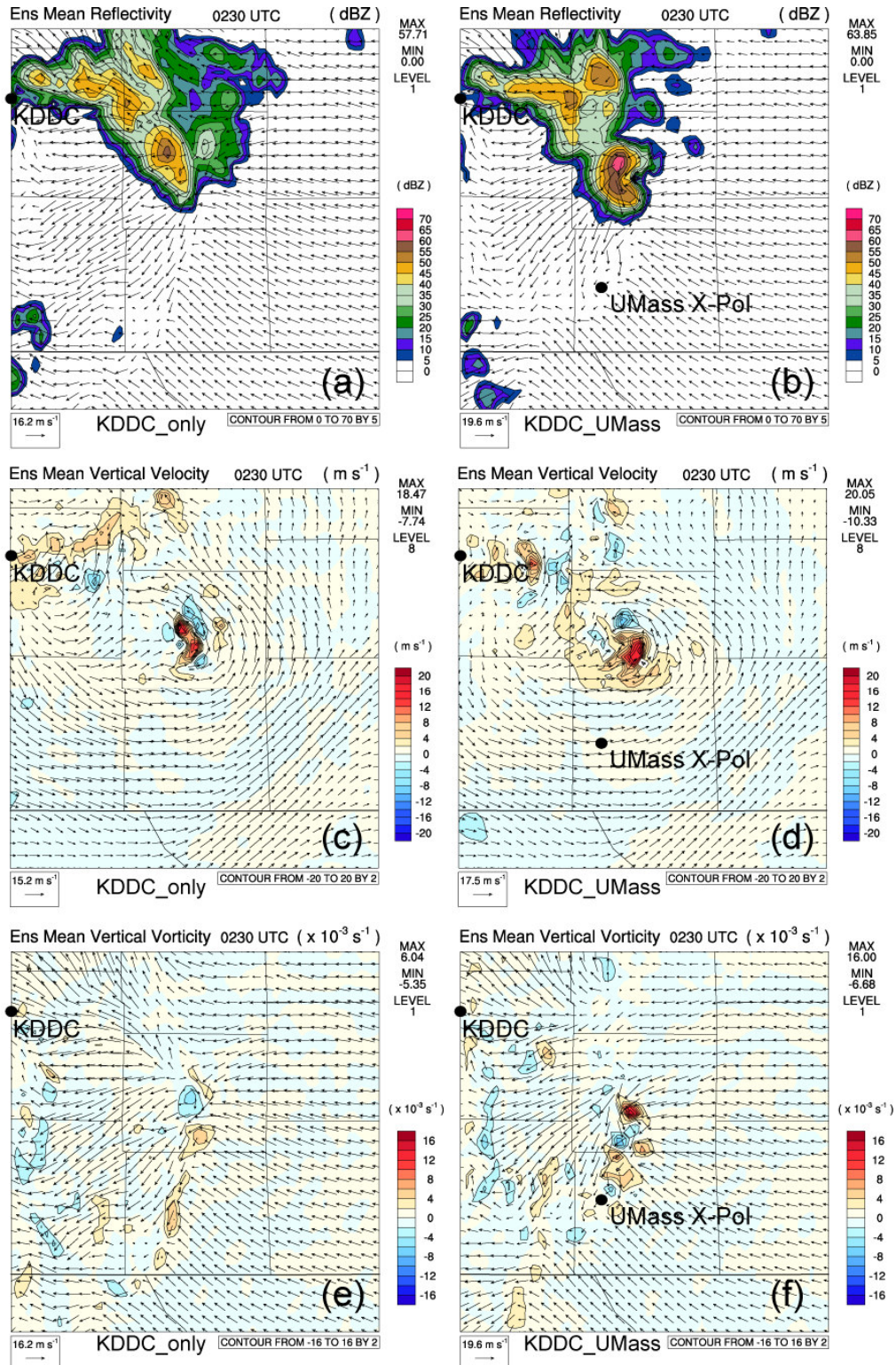


Fig. 7. Prior ensemble mean analysis fields at 0230 UTC for (left column) KDDC_only and (right column) KDDC_UMass experiments: (a, b) calculated reflectivity (in dBZ) at 228 m; (c, d) vertical velocity (in m s⁻¹) at 4 km; and (e, f) vertical vorticity (in 10⁻³ x s⁻¹) at 228 m. Horizontal velocity vectors (in m s⁻¹) are storm relative, assuming a storm motion of (U, V) = (6.0 m s⁻¹, 9.0 m s⁻¹).

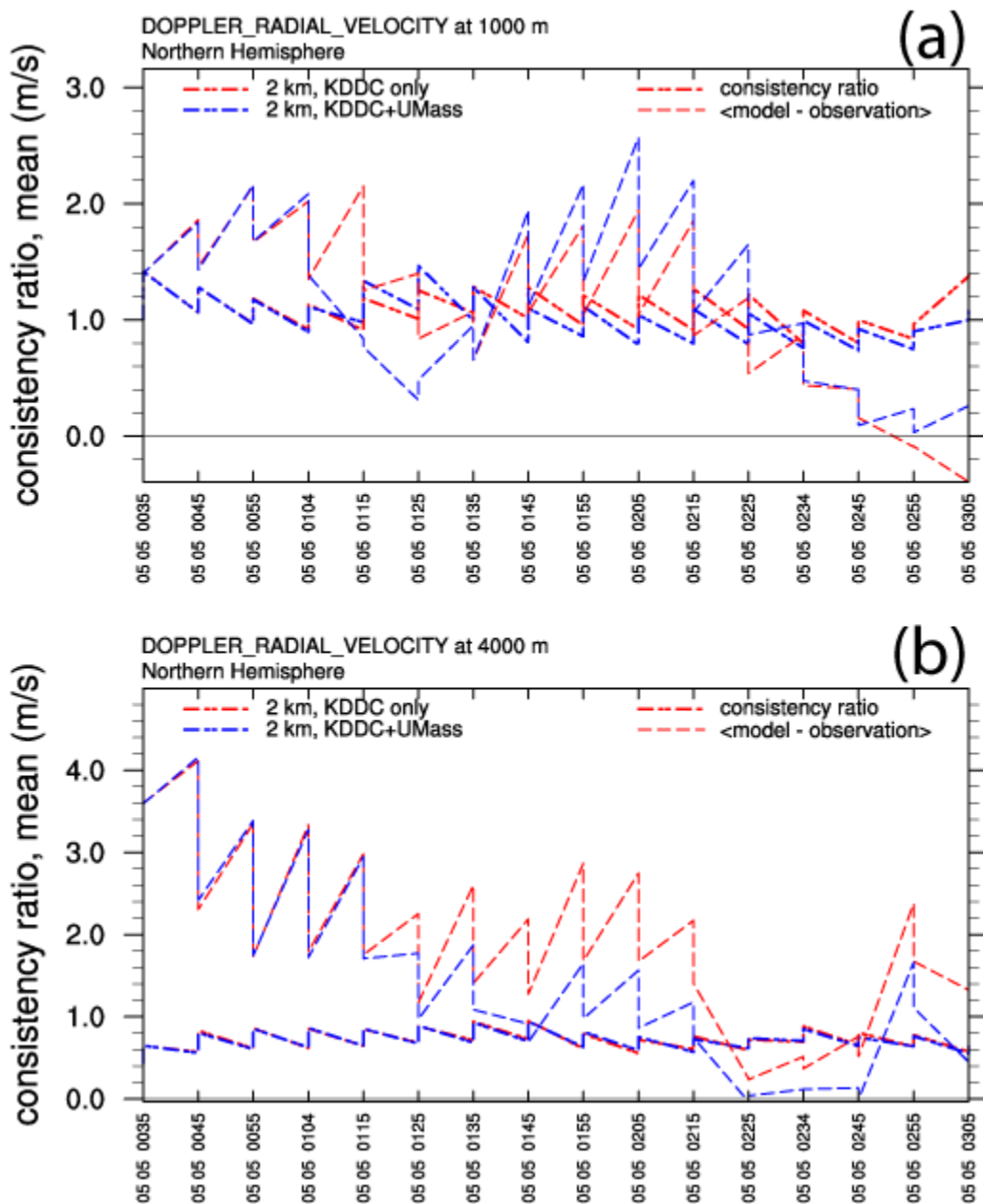


Fig. 8. Observation-space diagnostics, over 10-minute intervals, for the KDDC_only (red) and KDDC_UMass (blue) experiments for (a) 0 – 1000 m AGL, (b) 3000 – 4000 m AGL. The consistency ratio is plotted in the thick dot-dash line, and the volume-averaged innovation is plotted in the thin dashed line. Both prior and posterior quantities are plotted, hence the “sawtooth” pattern.